

Hydraulic conductivity estimation by considering the existence of piles: A case study

Yao Yuan^{1,2a}, Ye-Shuang Xu^{*1,2}, Jack S. Shen^{1,3b} and Bruce Zhi-Feng Wang^{4c}

¹State Key Laboratory of Ocean Engineering and Collaborative Innovation Center for Advanced Ship and Deep-Sea Exploration (CISSE), Department of Civil Engineering, Shanghai Jiao Tong University, Shanghai 200240, China

²Key Laboratory of Land Subsidence Monitoring and Prevention, Ministry of Land and Resources, and Shanghai Engineering Research Center of Land Subsidence, Shanghai 200072, China

³Department of Civil and Construction Engineering, Swinburne University of Technology, Hawthorn, Victoria 3122, Australia

⁴Department of Geotechnical and Tunnelling Engineering, School of Highway, Chang'an University, Xi'an, Shanxi 710064, China

(Received April 13, 2016, Revised March 20, 2017, Accepted September 20, 2017)

Abstract. Estimation of hydraulic parameters is a critical step during design of foundation dewatering works. When many piles are installed in an aquifer, estimation of the hydraulic conductivity should consider the blocking of groundwater seepage by the piles. Based on field observations during a dewatering project in Shanghai, hydraulic conductivities are back-calculated using a numerical model considering the actual position of each pile. However, it is difficult to apply the aforementioned model directly in field due to requirement to input each pile geometry into the model. To develop a simple numerical model and find the optimal hydraulic conductivity, three scenarios are examined, in which the soil mass containing the piles is considered to be a uniform porous media. In these three scenarios, different sub-regions with different hydraulic conductivities, based on either automatic inverted calculation, or on effective medium theory (EMT), are established. The results indicate that the error, in the case which determines the hydraulic conductivity based on EMT, is less than that determined in the automatic inversion case. With the application of EMT, only the hydraulic conductivity of the soil outside the pit should be inverted. The soil inside the pit with its piles is divided into sub-regions with different hydraulic conductivities, and the hydraulic conductivity is calculated according to the volume ratio of the piles. Thus, the use of EMT in numerical modelling makes it easier to consider the effect of piles installed in an aquifer.

Keywords: piles; aquifer; dewatering; hydraulic conductivity; numerical model; EMT

1. Introduction

The Quaternary deposit in Shanghai has a thickness of more than 300 m and is composed of an alternated multi-aquifer-aquitard system (Xu *et al.* 2009, 2012, Zhu *et al.* 2016), which is a common aquifer system in many coastal areas (Cheng and Chen 2007, Hugman *et al.* 2015, Zhou X. 2016). The multi-aquifer-aquitard system generally has high hydraulic heads and is rich in groundwater. Underground spaces are developing with the increasing population and urbanization in coastal regions (Carlson *et al.* 2011, Jiao *et al.* 2006, 2008, Yin *et al.* 2014, 2015, Wu *et al.* 2015a, Zhang *et al.* 2015, 2017). For example, in Shanghai the number, and buried depth, of deep excavations are increasing Wang *et al.* 2012, 2013, Tan and Wang 2013a, b, Zhou *et al.* 2010). When excavations reach a depth of

around 20 m, where the first confined aquifer exists, geohazards such as quicksand, boiling, and piping may occur (Xu *et al.* 2009, Shen and Xu 2011, Wu *et al.* 2015a-e). Groundwater levels with high hydraulic heads in some coastal cities, such as, Barcelona (Pujades *et al.* 2014), Hong Kong (Forth 2004), Taipei (Ni *et al.* 2011), Tianjin (Shen *et al.* 2015a), and Shanghai (Xu *et al.* 2013, 2016, Ma *et al.* 2014, Wu *et al.* 2016), have been lowered during excavation by dewatering inside, or outside, the foundation pit to prevent these possible geohazards. Rapidly significant dropdown in water level due to dewatering would cause remarkable consolidation-induced ground settlement, which could cause permanent damage to superstructure or buried infrastructure in the proximity of pit (e.g., Tan *et al.* 2016, Tan and Lu 2016). Estimation of the hydraulic parameters of the soil is crucial for the analysis of excavation dewatering (Lin *et al.* 2010, Wu *et al.* 2013, Shen *et al.* 2014, 2015b). Pumping tests are conducted before dewatering, and these are a common method of determining hydraulic parameters in aquifers (Ni *et al.* 2011, 2013). Back-analysis, by fitting the modelling results and measured data based on pumping tests through an analytical method or a numerical method, is conducted to estimate hydraulic parameters such as hydraulic conductivity and specific storage (Johnson *et al.* 2002, Zhou *et al.* 2012, Wu *et al.* 2015b, c, Cai *et al.* 2014, Yoon *et al.* 2015). As

*Corresponding author, Associate Professor

E-mail: xuyeshuang@sjtu.edu.cn

^aPh.D. Student

E-mail: yuanyao12@sjtu.edu.cn

^bProfessor

E-mail: sshen@swin.edu.au

^cAssociate Professor

E-mail: zhifeng.wang@chd.edu.cn

numerical methods are particularly useful in complicated geological environments, and can give more reliable hydraulic parameters, they have become more widely used (Pujades *et al.* 2014, Wu *et al.* 2015c).

Many underground structures, such as diaphragm walls (Wang *et al.* 2012, Shen *et al.* 2013, Wu *et al.* 2016), tunnels (Han *et al.* 2016, 2017, Ye *et al.* 2015) and vertical barriers for contaminant (Anderson and Mesa 2006, Fan *et al.* 2014, Du *et al.* 2014a, b, 2015a, b, Richardson and Nicklow 2002) are, or will be, constructed in aquifer layers. The permeability, affecting the performance of these underground structures, had been widely investigated; and a series of empirical equations using property indexes were developed for prediction of the hydraulic conductivity (Hinchberger *et al.* 2010, Pujades *et al.* 2012a, Du *et al.* 2015a, b). The permeability of these underground structures required to be lower than 10^{-8} m/s for anti-seepage in general. Slurry-trench cutoff wall for groundwater containment as an example, Du *et al.* (2015b) indicated that the cutoff wall created using clayey-soil and 10% calcium bentonite (by dry weight) ensured a hydraulic conductivity lower the typical regulatory limit of 10^{-9} m/s. Using the predicting method proposed by Du *et al.* (2015a, b), the permeability of slurry walls can be well estimated with satisfactory accuracy. Due to the low-permeability characteristics of underground structures, the seepage behavior of the aquifer may change with the installation of underground structures (Mulligan *et al.* 2001, Ranjan *et al.* 2008, Vilarrasa *et al.* 2011, Pujades *et al.* 2012b). Piles are often constructed before excavation and dewatering to improve the soil due to poor geotechnical conditions. To consider the impact of the piles on dewatering, the influence region should be divided into sub-regions. The hydraulic parameters of the soil layers in different sub-regions should be respectively inverted using a numerical method, which makes the inversion results less certain. To analyze the blocking effect of underground structures on groundwater seepage, effective medium theory (EMT) is adopted to evaluate the equivalent hydraulic conductivity k_{eq} of an inhomogeneous medium (Dagan 1979, Frippiat and Holeyman 2008, Bunn *et al.* 2010). Since EMT is based on soft deposits with different sizes of randomly distributed soil blocks, the applicability of EMT to the estimation of k_{eq} of an aquifer, taking into account piles embedded at regular intervals, should be confirmed through practical application. Here, a case study of foundation pit dewatering in Shanghai is presented. A numerical simulation was conducted to deduce the hydraulic conductivity of the aquifer. The objective of this study is to demonstrate the feasibility of EMT for the estimation of the hydraulic conductivity of aquifers containing piles, and to evaluate the optimal value of hydraulic conductivity with consideration of the effect of piles on groundwater seepage during foundation pit dewatering.

2. Brief review of EMT

The EMT method is adopted to estimate k_{eq} in an inhomogeneous medium (Ding *et al.* 2008, Du *et al.* 2014, Yin *et al.* 2016, Xu *et al.* 2014). The inhomogeneous

medium is assumed to consist of homogeneous blocks of high hydraulic conductivity with several other blocks of lower hydraulic conductivity embedded therein. The distant groundwater boundary is assumed to be far from the inclusions (Xu *et al.* 2012, Ma *et al.* 2014, Ding *et al.* 2008). Therefore the groundwater seepage follows a steady flow around the embedded material. The other assumption is that the effects of different inclusions on the hydraulic gradient are isolated.

The value of k_{eq} can be calculated as follows (Dagan 1979)

$$k_{eq} = \frac{1}{D} \left[\int_0^\infty \frac{V(k)dk}{k(D-1) + k_{eq}} \right]^{-1} \quad (1)$$

where k_{eq} =equivalent hydraulic conductivity, k =hydraulic conductivity of different medium, $V(k)$ =probability density function of the hydraulic conductivity, and D =spatial dimension.

In the case of binary media, (i.e., the soil and the piles), Eq. (1) becomes (Renard and Marsily 1997)

$$k_{eq} = \frac{1}{D} \left[\frac{V_s}{k_s + k_{eq}(D-1)} + \frac{V_b}{k_b + k_{eq}(D-1)} \right]^{-1} \quad (2)$$

where V_s =volume ratio of natural soil, V_b =volume ratio of piles to the soil, k_s = hydraulic conductivity of the soil, and k_b =hydraulic conductivity of the piles. The aforementioned equation is valid when V_b is less than 0.6 (Desbarats 1992).

Based on Eqs. (1) and (2), the volume ratio of the piles to the soil is considered in the estimation of equivalent hydraulic conductivity. Here, the EMT method is applied to estimate k_{eq} of the aquifer with piles installed therein.

3. Project overview

The Shanghai Grand Centre, with an area of 9,785.9 m², is located in the Pudong New Area of Shanghai, and it is enclosed by Century Boulevard, Xiangcheng Road, and Fushan Road. Fig. 1 shows a plan view of the project. This project includes a main building and a low-level skirting building. Shanghai Metro Lines No. 2, 4, and 9 pass through within the vicinity of this project. Fig. 2 shows a plan view of the foundation pit and piles. The absolute elevation of the ground is +5.00 m. The foundation pit was divided into three excavated regions (I, II, and III). The excavated depth of the main building is 22.25 m, that of the skirting building is 20.75 m, and that of the area near Shanghai metro line No. 4 is 17.05 m. Diaphragm walls, with a buried depth of 37.95 m to 41.00 m, and a width of 1000 mm to 1200 mm, were used as retaining structures. A large number of piles which were divided into two types-main bearing piles and basement uplift piles-had been installed in the foundation pit before the pumping tests (Table 1).

Fig. 3 shows the geotechnical profile and soil properties beneath the Shanghai Grand Centre. The soil within 120 m of the field site includes 12 layers as follows: fill (Layer 1), silty clay (Layer 2), silty clay (Layer 3), silty clay (Layer 4), clay (Layer 5-1), silty clay Layer 5-2, silty clay (Layer 6), sandy silt (Layer 7-1), silt (Layer 7-2), silt (Layer 9-1), fine sand (Layer 9-2), and silty clay (Layer 11). The detailed

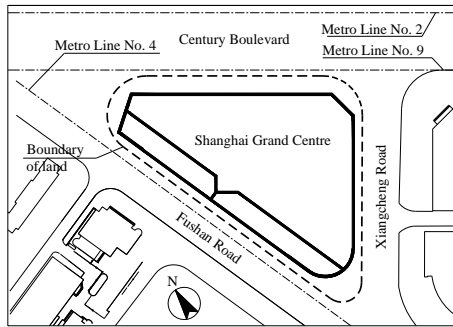


Fig. 1 Plan view of the Shanghai Grand Centre site

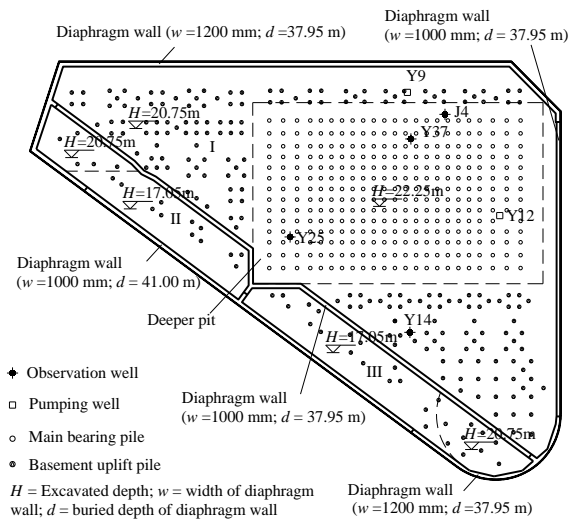


Fig. 2 Plan view of the piles and wells affecting the pumping test

Table 1 Distribution, and characteristics, of the piles

Type	Length (m)	Diameter (m)	Elevation (m)		Buried depth (m)		Number
			Top	Bottom	Top	Bottom	
Main bearing pile (Pile I)	49.90	0.8	-18.05	-67.95	23.05	72.95	322
Basement uplift pile (Pile II)	30.00	0.8	-16.55	-46.55	21.55	51.55	232

description of Shanghai ground can be referred to the studies of Wu *et al.* (2015) and Ye and Ye (2016). Soil layers 7, 9, and 11 in Fig. 3 correspond to the first confined aquifer layer (AqI), the second confined aquifer layer (AqII), and the third confined aquifer layer (AqIII) in Shanghai (SUCCC, 2010). The buried depth of groundwater level in the phreatic aquifer is 0.50 m. Some aquitard layers are absent from this field site, so AqI, AqII, and AqIII are interconnected and a composite confined aquifer group is formed. The depth to this composite confined aquifer group is 26.00 to 27.00 m, and the depth to the groundwater level is 9.00 m. The presence of the confined aquifer group is potentially harmful to the stability of the foundation pit because of the high water pressure.

Table 2 Characteristics of the test-wells used in the simple pumping test

Well no.	Type	Depth of hole (m)	Length of well (m)	Buried depth of gravel fill (m)	Buried depth of filter tube (m)	Static pressure water depth (m)	Soil layer
Y9	Pumping well	42	32	29-42	31-41	8.90	
Y12	pumping well	40	30	27-40	29-39	8.90	
Y14	observation well	42	32	29-42	31-41	9.07	Layer 7-1 & 7-2
Y25	observation well	42	32	29-42	31-41	8.81	
Y37	observation well	42	32	29-42	31-41	9.15	
J4	observation well	37	32	30-37	31-36	9.12	

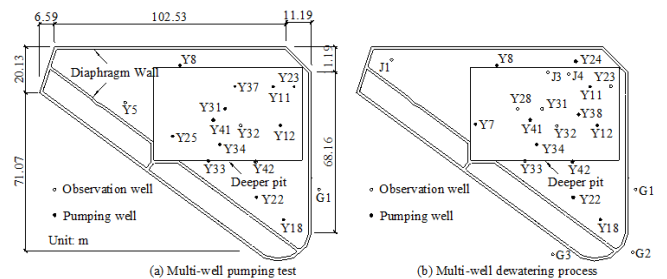


Fig. 4 Plan view of the wells used in the multi-well pumping test and dewatering process

Table 3 Characteristics of the pumping wells used in the multi-well pumping test and the dewatering process

Well no.	Depth of hole (m)	Length of well (m)	Buried depth of gravel fill (m)	Buried depth of filter tube (m)	Pumping period	Soil layer
Y23	37	28	25-38	27-37		
Y25	42	32	29-42	31-41		
Y31	42	32	29-42	31-41		Multi-well pumping test
Y33	42	32	29-42	31-41		
Y37	42	32	29-42	31-41		
Y8	40	30	27-40	29-39		
Y11	40	30	27-40	29-39		Layer 7-1 & 7-2
Y12	40	30	27-40	29-39		Multi-well pumping test & Dewatering process
Y18	40	30	27-40	29-39		
Y22	42	32	29-42	31-41		
Y34	42	32	29-42	31-41		
Y41	42	32	29-42	31-41		

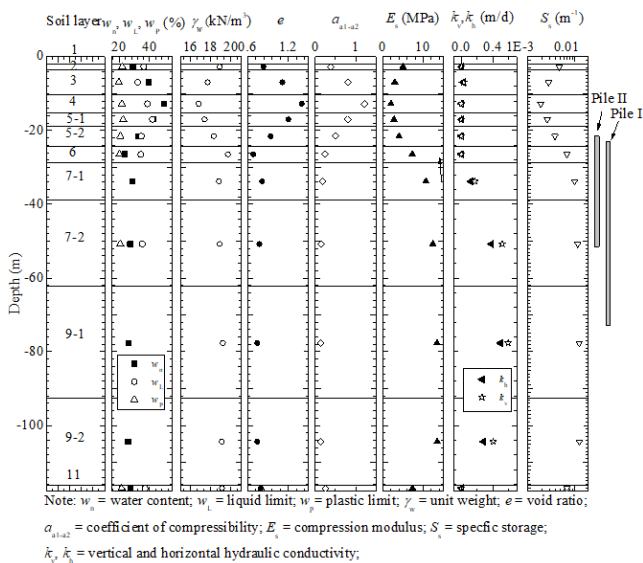


Fig. 3 Geotechnical profile and soil properties in Shanghai Grand Centre

Table 3 Continued

Well no.	Depth of hole (m)	Length of well (m)	Buried depth of gravel fill (m)	Buried depth of filter tube (m)	Pumping period	Soil layer
Y42	42	32	29-42	31-41	Dewatering process	
Y7	42	32	29-42	31-41		
Y24	40	30	27-40	29-39		
Y38	42	32	29-42	31-41		

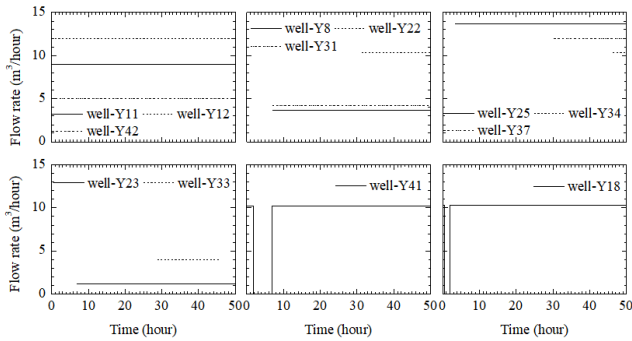


Fig. 5 Flow rates from the pumping wells during the multi-well pumping test

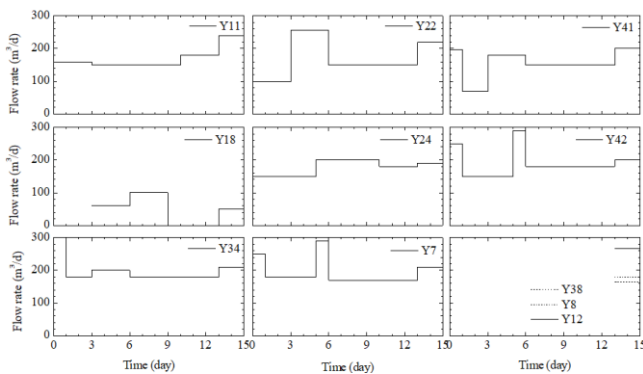


Fig. 6 Flow rate of the pumping wells during the dewatering process

4. Well pumping test and multi-well dewatering process

In this case study two pumping tests were conducted, including a simple pumping test and a multi-well pumping test. First a simple pumping test was conducted to deduce the hydraulic parameters. Then a multi-well pumping test was conducted to verify the deduced hydraulic parameters and to estimate the drawdown of the groundwater level. A formal multi-well dewatering process was carried out after the pumping test.

4.1 Simple pumping test

A simple pumping test was conducted before the multi-well pumping test in the Shanghai Grand Centre. As shown in Fig. 2, there were six test-wells (wells Y9, Y12, Y14, Y25, Y37, and J4) used in this project. Table 2 shows the characteristics of these test-wells. Wells Y9 and Y12 are pumping wells and wells J4, Y14, Y25, and Y37 are observation wells. The average static groundwater level is -9.00 m. Groundwater was pumped from wells Y9 and Y12

simultaneously during the simple pumping test. The water output was 17.0 m³/h from well Y9 and 6.2 m³/h from well Y12. The groundwater level in the observation wells remained stable after 22 hours of pumping. After the pumping test, the stable groundwater levels in observation wells Y14, Y25, Y37, and J4 were -11.72 m, -11.44 m, -14.09 m, and -13.97m, with groundwater drawdowns of 2.65 m, 2.61 m, 4.94 m, and 4.85 m, respectively.

4.2 Multi-well pumping test

The multi-well pumping test was conducted before the dewatering process in this study. As shown in Fig. 4, thirteen pumping wells and three observation wells were opened during the multi-well pumping test. The structure of the pumping wells is similar to those used in the simple pumping test. Table 3 shows the characteristics of the pumping wells in the multi-well pumping test. Fig. 5 shows the flow rates from each of the pumping wells.

4.3 Multi-well dewatering process

Only the first 15 days of the dewatering process were analyzed: eleven pumping wells were used as shown in Fig. 4. There were eight observation wells inside the pit and three observation wells outside the pit. The characteristics of the pumping wells are also shown in Table 3. Fig. 6 shows the flow rate from the pumping wells during the dewatering process over the first 15 days.

5. Numerical simulation

5.1 Numerical model

Based on the geological conditions, the foundation pit, and the multi-well pumping test, a three-dimensional finite difference model (FDM) was established. The analysis range is determined by the influencing radius R of the simple pumping test in the confined aquifer, which can be calculated by using Thiem's equation. The maximum calculated value of R is 419.3 m. Fig. 7 shows the three-dimensional (3-d) finite difference mesh used for the modelling. It measures 3000 m in the x -direction by 3000 m in the y -direction. The maximum horizontal mesh interval is set to 120×120 m, while the mesh intervals around the foundation pit are more refined and measure 1 × 0.8 m. The numbers of nodes and elements in each layer are 41,200 and 40,795, respectively. The analysis depth in the vertical direction is 150 m and the geological system includes 15 strata. Fig. 8 shows the finite element mesh around the foundation pit. To check the effect of the size and shape of the mesh on the numerical results, a sensitivity analysis was conducted by comparing several schemes with different sizes and shapes of mesh. The adopted scheme for mesh size and shape was found to have been sufficiently accurate.

The diaphragm wall is represented by an impermeable medium. The initial groundwater level of the phreatic aquifer and the confined aquifer were set to -1.00 m and -9.00 m, respectively. The four boundaries of this model are set as fixed hydraulic head boundaries. The initial parameters are summarized in Fig. 3.

In this case study, many piles were constructed in the

foundation pit before the pumping tests. The blocking effect of the piles on groundwater seepage from aquifers should be considered. To obtain the optimal hydraulic parameters by considering the influence of the piles, piles are represented by impermeable elements inside the foundation pit according to the actual position of the piles. The hydraulic parameters of the same soil layer inside, and outside, the foundation pits are the same, and should be inverted in the numerical simulation. This scenario considers the actual position of the piles (labelled as Case I).

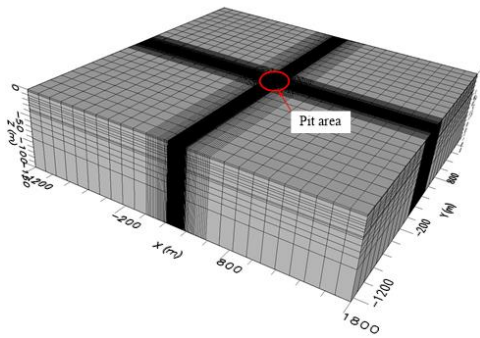


Fig. 7 3-d finite difference mesh

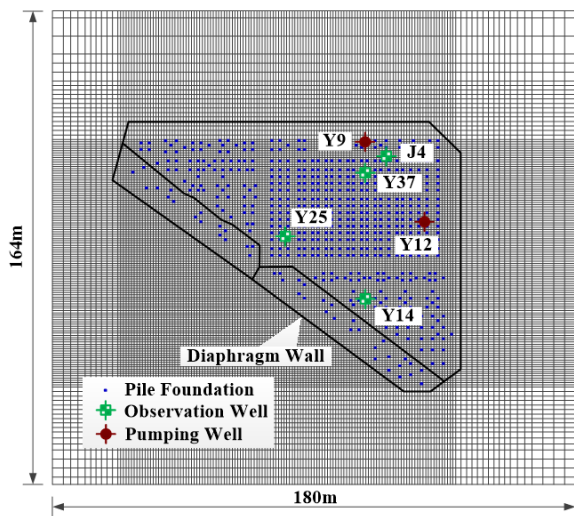


Fig. 8 Plan view of fine finite difference mesh around the foundation pit

Table 4 Inverted parameters in the numerical model for Case I

Calculated layer	Soil layer	Buried depth (m)	k_x	k_y	k_z	S_S	n
1	1	0~1.89	0.001	0.001	0.0006	1E-6	0.3
2	2	1.89~3.51	0.001	0.001	0.0006	1E-6	0.3
3	3	3.51~10.36	0.001	0.001	0.0006	1E-6	0.3
4	4	10.36~15.18	0.001	0.001	0.0006	1E-6	0.3
5	5-1	15.18~18.8	0.001	0.001	0.0006	1E-6	0.3
6	5-2	18.8~24.3	0.0002	0.0002	4E-5	1E-6	0.1
7	6	24.3~28.65	0.0002	0.0002	4E-5	0.0001	0.1
8							
9	7-1	28.65~37.0	3.6	3.6	0.5	0.0001	0.1

Table 4 Continued

Calculated layer	Soil layer	Buried depth (m)	k_x	k_y	k_z	S_S	n
10							
11	7-2	37.0~62.5	3.8	3.8	0.12	8E-5	0.1
12							
13	9-1	62.5~82.5	10.6	10.6	2	5E-5	0.1
14							
15	9-2	82.5~152	19.2	19.2	4	5E-5	0.2

*Note: k_x and k_y are the horizontal hydraulic conductivities in the x - and y -directions (m/d), k_z is the vertical hydraulic conductivity (m/d), S_S is the specific storage (1/m), n is the porosity

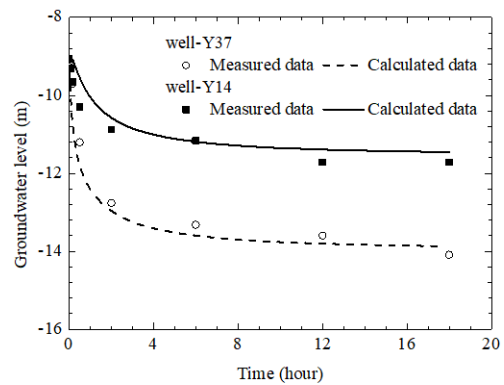


Fig. 9 Comparison of groundwater levels inside the foundation pit: The simple pumping test

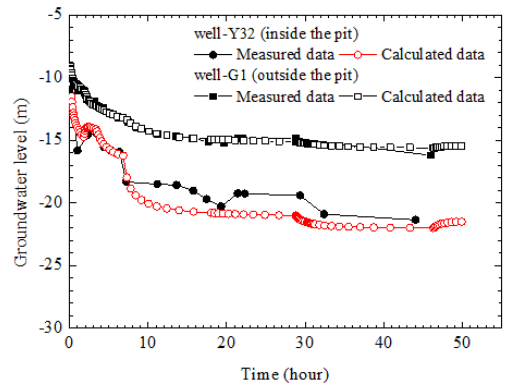


Fig. 10 Comparison of groundwater levels inside, and outside, the foundation pit: Multi-well pumping test

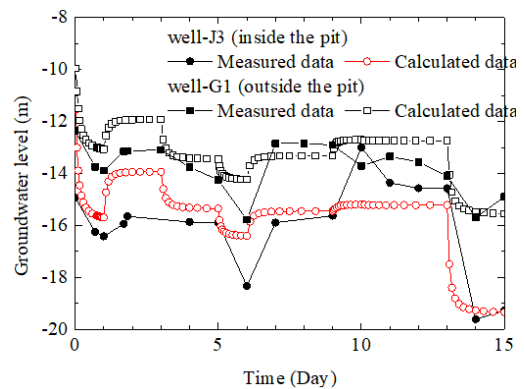


Fig. 11 Comparison of groundwater levels inside, and outside, the foundation pit: Dewatering process

5.2 Estimation of hydraulic parameters

The hydraulic parameters of the aquifer should be repeatedly corrected by comparison between the field pumping test results and the numerical analysis results to minimise the errors therein. The hydraulic parameters are deduced from pumping test data. The modified seepage parameters obtained by back-analysis are then used for the design of the dewatering operation (Li *et al.* 2002, Liu *et al.* 2003, Jin *et al.* 2016a, b).

The deduced hydraulic parameters of the aquifer layers in Case I are summarized in Table 4. Fig. 9 shows a comparison of the calculated, and measured, groundwater levels for the simple pumping test. To calibrate the reliability of the groundwater model, the least squares method is used to minimize the sum of the squared errors. The estimated standard error of the groundwater level between the calculated results and the measured data in Case I is 0.125 m, which indicates that this deduced parameter in Case I is valid for the simple pumping test. The applicability of the deduced hydraulic conductivity should be further examined in the dewatering process.

5.3 Verification of hydraulic parameters

To verify the hydraulic parameters, the deduced hydraulic parameters were used to simulate the previously mentioned multi-well pumping test and dewatering process. The maximum calculated value of R is 356.6 m for the multi-well pumping test and 383.2 m for the dewatering process, which are both smaller than those values from the simple pumping test. The numerical model of the multi-well pumping test and the dewatering process give values that are the same as those of the simple pumping test. Figs. 10 - 11 show a comparison of the groundwater levels for the multi-well pumping test and the dewatering process. The measured data and numerical results suffer some omissions during dewatering process because the hydraulic conductivity is set as a mean average value in the numerical analysis, while in fact the hydraulic conductivities of the aquifers are variable. Meanwhile, in the numerical analysis, only the dewatering effect is considered but the excavation effect which may disturb the soil and impact the hydraulic conductivity of the aquifers is ignored. The numerical results fit the measured data better inside the pit than outside. The estimated standard error of the calculated result and the measured result for Case I is 0.285 for the multi-well pumping test, and 0.62 m for the dewatering process.

6. Results and discussion

It is necessary to find a balance between performance and complexity in the selection and calibration of a groundwater model (Schöniger *et al.* 2015). As each pile should be set in the finite model for Case I, which considers the actual position of the piles, the model for Case I is more complex, which is impractical. To find the most applicable numerical model and the corresponding optimal hydraulic parameters, three scenarios have been considered before making any comparison with Case I. The finite model for

the following three scenarios is the same, but the division of hydraulic conductivities is different (Fig. 12).

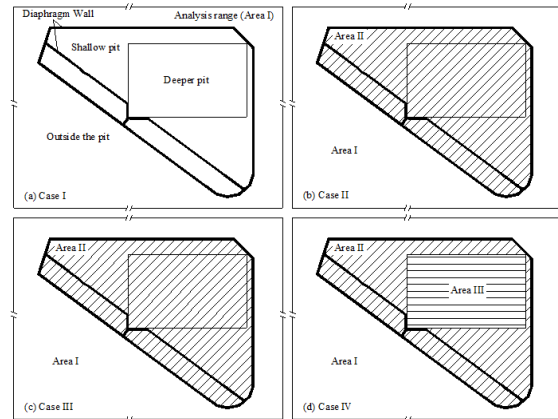


Fig. 12 Division of hydraulic conductivities: Cases I to IV

Table 5 EMT parameters

Case	Soil layer	Buried depth (m)	D	V_s	V_b		
Case III	Area II	7-1	33.65-42.0	3	96.3%	3.7%	
		7-2	42.0-51.6	3	96.3%	3.7%	
				51.6-67.5	3	97.7%	2.3%
Case IV	Area II	7-1	33.65-42.0	3	97.7%	2.3%	
		7-2	42.0-51.6	3	97.7%	2.3%	
				51.6-67.5	3	100%	0
	Area III	7-1	33.65-42.0	3	93.1%	6.9%	
		7-2	42.0-51.6	3	93.1%	6.9%	
				51.6-67.5	3	94.6%	5.4%

Table 6 Deduced hydraulic conductivity of the aquifer layers (used in the numerical model)

Soil layer	Buried depth (m)	Case	Hydraulic conductivity					
			k_x	k_y	k_z			
7-1	28.65~37.0	Case I	Area I	3.6	3.6	0.5		
			Area II	2.88	2.88	0.1		
		Case II	Area I	3.28	3.28	0.1		
			Area II	3.4	3.4	0.5		
		Case III	Area I	3.6	3.6	0.5		
			Area III	3.23	3.23	0.5		
		Case IV	Area II	3.47	3.47	0.5		
			Area I	3.6	3.6	0.5		
		7-2	37.0~51.6	Case I	Area I	3.8	3.8	0.12
					Area II	3	3	0.216
				Case II	Area I	3.4	3.4	0.216
					Area II	3.59	3.59	0.12
Case III	Area I			3.8	3.8	0.12		
	Area III			3.407	3.407	0.12		
Case IV	Area II			3.67	3.67	0.12		
	Area I			3.8	3.8	0.12		

Table 6 Continued

Soil layer	Buried depth (m)	Case	Hydraulic conductivity			
			k_x	k_y	k_z	
7-2	51.6~62.5	Case I	Area I	3.8	3.8	0.12
			Area II	3.1	3.1	0.216
		Case II	Area I	3.4	3.4	0.216
			Area II	3.67	3.67	0.12
		Case III	Area I	3.8	3.8	0.12
			Area III	3.49	3.49	0.12
		Case IV	Area II	3.8	3.8	0.12
			Area I	3.8	3.8	0.12

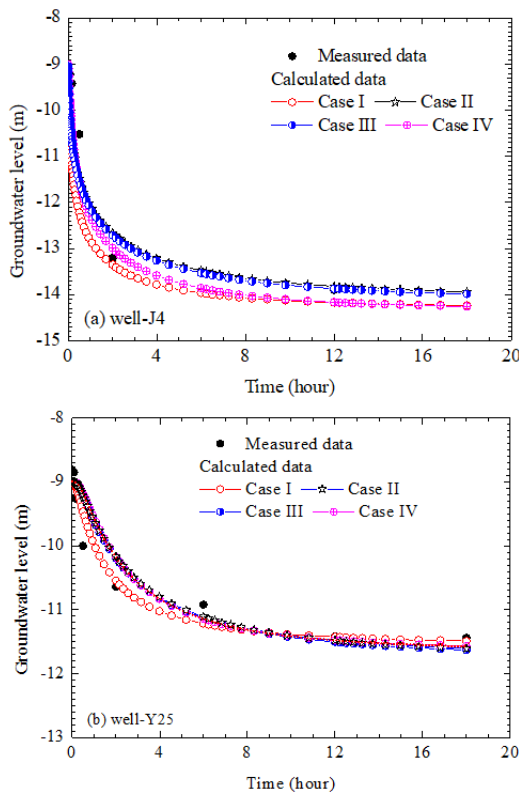


Fig. 13 Comparison of groundwater levels inside the foundation pit: Simple pumping test

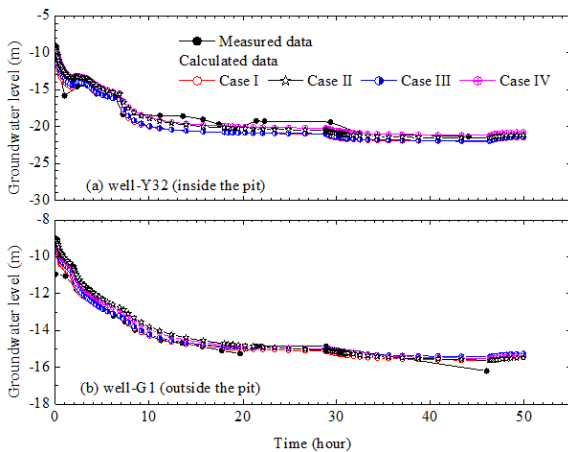


Fig. 14 Comparison of groundwater levels inside, and outside, the foundation pit: Multi-well pumping test

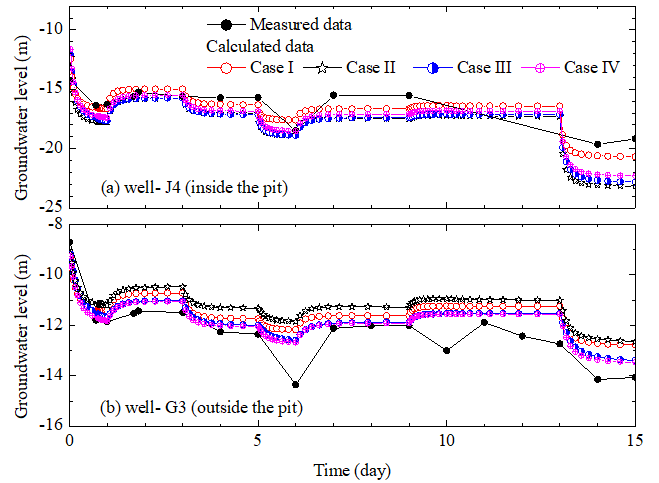


Fig. 15 Comparison of groundwater levels inside, and outside, the foundation pit: Dewatering process

Table 7 Error analysis for the calculated, and measured, data for the four multi-well pumping test cases and the dewatering process

Pumping period	Case	Maximum error (m)	Minimum error (m)	Average error (m)	Estimated standard error (m)
Multi-well pumping test	I	0.766	-0.028	0.200	0.285
	II	0.956	-0.034	0.278	0.340
	III	0.732	0.229	0.201	0.310
	IV	0.841	0.139	0.536	0.208
Dewatering process	I	-4.757	-0.065	-1.073	0.620
	II	-7.422	-0.830	-3.024	0.835
	III	-7.031	-0.619	-2.995	0.732
	IV	-6.539	-0.208	-2.602	0.690

Case II: this case does not consider the actual position of the piles. The aquifer soil with piles inside the foundation pit was considered to be a uniform porous material. Therefore, the hydraulic conductivity of the same soil layer was divided into two areas including Area I outside, and Area II inside, the foundation pit. The hydraulic conductivities of Areas I and II are then inverted by the numerical simulation.

Case III: this case also does not consider the actual position of piles. The finite model and division of hydraulic conductivities in this case are the same as in Case II.

The difference between Case II and Case III lies in the setting of the value of hydraulic conductivity. The hydraulic conductivity of Area III was calculated according to the hydraulic conductivity of Area I, and the volume ratio of piles inside the foundation pit was based on the EMT. In Case III, the hydraulic conductivity in Area I outside the pit is equal to the inverted hydraulic conductivity from Case I.

Case IV: the finite model of this case is also the same as that for Case II. The hydraulic conductivity of the same soil layer was divided into three areas including Area I outside the pit, Area II in the shallow pit, and Area III in the deeper part of the pit. The hydraulic conductivities of Areas II and III were calculated based on the hydraulic conductivity of Area I, and the volume ratio of piles in the shallow and

deeper parts of the pit were both based on EMT. In Case IV, the hydraulic conductivity of Area I outside the pit is equal to the inverted hydraulic conductivity from Case I.

According to the sensitivity analysis, the hydraulic conductivity of soil layers 7-1 and 7-2 are the parameters which exert the greatest influence on the simulated results. Repeated tentative calculations and comparison of results for the hydraulic conductivity of soil layers 7-1 and 7-2 is necessary. Other hydraulic parameters should not need repeated iteration because their influence on the stable groundwater level is small. The parameters of Case II to Case IV are therefore chosen to be the same as those of Case I, except for the hydraulic conductivity of layers 7-1 and 7-2. Since the buried depth of pile I and pile II are different, soil layer 7-2 is divided into two layers in the numerical model at a depth of 51.6 m, which is approximately equal to the buried depth of the toe of pile II. The hydraulic conductivity of layer 7-2 above 51.6 m is evaluated by considering the impact of pile I and pile II while below 51.6 m only the impact of pile I is considered. Table 5 lists the EMT parameters used for Cases III and IV. Table 6 summarizes a comparison of the deduced hydraulic parameters of layers 7-1 and 7-2 for the four scenarios: because of the blocking effect of the piles on groundwater seepage, the hydraulic conductivity inside the pit is less than that outside the pit in Cases II and III. For Case IV, the hydraulic conductivity in the deeper pit is less than that in the shallow pit because the distribution of piles in the deeper pit is more dense.

Fig. 13 shows a comparison of the calculated and measured groundwater level for the simple pumping test. The estimated standard error of the calculated results, and measured data, for the four cases is similar, with values of 0.125, 0.100, 0.125, and 0.120 m, respectively, which indicates that the deduced parameters for the four scenarios are valid for the simple pumping test. However the value of the deduced hydraulic parameters of layers 7-1 and 7-2 inside, and outside, the pit in the four scenarios differs. The applicability of the deduced hydraulic conductivity should be further examined in the multi-well pumping test and the dewatering process, and the optimal hydraulic conductivity should be selected.

Figs. 14 and 15 show a comparison of the groundwater levels inside, and outside, the foundation pit for the multi-well pumping test and for the dewatering process, respectively. The difference between the calculated data from the four scenarios and the measured data inside the pit is smaller than that outside the pit. The groundwater level inside the pit calculated from the four scenarios is similar to that outside pit, but the difference in level outside the pit is more marked. Table 7 summarizes an error analysis for the four cases. The estimated standard errors of the calculated result and the measured result for the four cases are 0.285, 0.34, 0.31, and 0.208 for the multi-well pumping test, and 0.62, 0.835, 0.732, and 0.69 m for the dewatering process. The error for Case II is the largest. The errors for Cases I and IV are relatively low.

Although the hydraulic conductivity inverted from Case I is the most reliable value based on its exhibiting the least error, the models for Cases II to IV are simpler than the model for Case I, which may make them more appropriate

in practical applications. As shown in Figs. 14 - 15, the results calculated from Case IV fit the measured data better than those from Cases II and III. Furthermore, the error in Case IV is less than those in Cases II and III. The hydraulic conductivity applied in Case IV is optimal when compared with those in Cases II and III, which indicates that the hydraulic conductivity calculated by EMT can be applied in practical dewatering projects.

According to EMT, if the hydraulic conductivity of the soil layer outside the pit is known, that inside the pit can be deduced. As the hydraulic conductivity inside the pit in Case IV is calculated based on that outside the pit, which itself is equal to the inverted value from Case I, it is also difficult to apply it directly in engineering practice; however, the concept underpinning EMT can be used in the inversion of hydraulic conductivity data. First, the initial division of the zone according to hydraulic conductivity considers both the inside and the outside of the pit. Further division inside the pit should then be conducted according to the position of piles in the foundation pit. Only the hydraulic conductivity outside the pit needs to be inverted during numerical simulation. The value of the hydraulic conductivity inside the pit can be calculated using EMT by inputting the pile volume ratio as a parameter. The back-calculated hydraulic conductivity based on EMT is more accurate.

7. Conclusions

Based on a case study involving a single-well pumping test and the multi-well dewatering process used in the Shanghai Grand Centre project, this study estimates hydraulic conductivities by taking into account the blocking effect on groundwater seepage induced by the piles using numerical modelling. The following conclusions can be drawn:

- Generally the aquifer soil containing piles is considered as being a uniform porous material in the numerical model. If the piles are installed inside the pit in practice, because of the blocking effect on groundwater seepage from piles, the hydraulic conductivity inside the pit is lower than that outside the pit. The hydraulic conductivity of the soil inside, and outside, the pit should be estimated.
- By comparing the four numerical simulation scenarios, the error in Case II is the largest. The results indicate that it is difficult to invert the optimal hydraulic conductivity inside, and outside, the pit automatically based on the pumping test.
- The concept of EMT can be applied to the inversion of the hydraulic conductivity by considering the blocking effect of piles on groundwater seepage. If the hydraulic conductivity outside the pit is known, the hydraulic conductivity of the soil with piles inside the pit can be calculated using EMT.
- By numerical simulation using EMT, only the hydraulic conductivity of the soil outside the pit (without piles) needs to be inverted in practice. The hydraulic conductivity is initially considered across two zones: inside, and outside, the pit. Further division inside the pit should then be undertaken according to the position of the piles in

the foundation pit. The hydraulic conductivity of the soil containing piles inside the pit is divided into sub-regions and calculated from the pile volume ratio. The artificial inverted hydraulic conductivity based on EMT is deemed to have been credible.

Acknowledgements

The research work described herein was funded by the National Nature Science Foundation of China (NSFC) (Grant No. 41472252) and supported by Key Laboratory of Land Subsidence Monitoring and Prevention, Ministry of Land and Resources in China (No. KLLSMP201502). These financial supports are gratefully acknowledged.

References

- Anderson, E.I. and Mesa, E. (2006), "The effects of vertical barrier walls on the hydraulic control of contaminated groundwater", *Adv. Water Resour.*, **29**(1), 89-98.
- Bunn, M.I., Jones, J.P., Endres, A.L. and Rudolph, D.L. (2010), "Effects of hydraulic conductivity heterogeneity on vadose zone response to pumping in an unconfined aquifer", *J. Hydrol.*, **387**(1-2), 90-104.
- Cai, G., Zhou, A. and Sheng, D. (2014), "Permeability function for unsaturated soils with different initial densities", *Can. Geotech. J.*, **51**(12), 1456-1467.
- Carlson, M.A., Lohse, K.A., Jennifer, C., McIntosh, J.C. and McLain, J.E. (2011), "Impacts of urbanization on groundwater quality and recharge in a semi-arid alluvial basin", *J. Hydrol.*, **409**(1-2), 196-211.
- Cheng, C. and Chen, X. (2007), "Evaluation of methods for determination of hydraulic properties in an aquifer-aquitard system hydrologically connected to a river", *Hydrogeol. J.*, **15**(4), 669-678.
- Dagan, G. (1979), "Models of groundwater flow in statistically homogeneous porous formations", *Water Resour. Res.*, **15**(1), 47-63.
- Desbarats, A.J. (1987), "Numerical estimation of effective permeability in sand-shale formation", *Water Resour. Res.*, **23**(2), 273-286.
- Ding, G.P., Jiao, J.J. and Zhang, D.X. (2008), "Modelling study on the impact of deep building foundations on the groundwater system", *Hydrol. Process.*, **22**(12), 1857-1865.
- Du, Y.J., Fan, R.D., Liu, S.Y., Reddy, K.R. and Jin, F. (2015a), "Workability, compressibility and hydraulic conductivity of zeolite-amended clayey soil/calcium-bentonite backfills for slurry-trench cutoff walls", *Eng. Geol.*, **195**, 258-268.
- Du, Y.J., Fan, R.D., Reddy, K.R., Liu, S.Y. and Yang, Y.L. (2015b), "Impacts of presence of lead contamination in clayey soil-calcium bentonite cutoff wall backfills", *Appl. Clay Sci.*, **108**, 111-122.
- Du, Y.J., Jiang, N.J., Liu, S.Y., Jin, F., Singh, D.N. and Puppala, A.J. (2014a), "Engineering properties and microstructural characteristics of cement-stabilized zinc-contaminated kaolin", *Can. Geotech. J.*, **51**(3), 289-302.
- Du, Y.J., Wei, M.L., Reddy, K.R., Liu, Z.P. and Jin, F. (2014b), "Effect of acid rain pH on leaching behavior of cement stabilized lead-contaminated soil", *J. Hazard. Mater.*, **271**, 131-140.
- Fan, R.D., Du, Y.J., Reddy, K.R., Liu, S.Y. and Yang, Y.L. (2014), "Compressibility and hydraulic conductivity of clayey soil mixed with calcium bentonite for slurry wall backfill: Initial assessment", *Appl. Clay Sci.*, **101**, 119-127.
- Forth, R.A. (2004), "Groundwater and geotechnical aspects of deep excavations in Hong Kong", *Eng. Geol.*, **72**(3), 253-260.
- Frippiat, C.C. and Holeyman, A.E. (2008), "A comparative review of upscaling methods for solute transport in heterogeneous porous media", *J. Hydrol.*, **362**(1-2), 150-176.
- Han, L., Ye, G.L., Chen, J.J., Xia, X.H. and Wang, J.H. (2017), "Pressures on the lining of a large shield tunnel with a small overburden: A case study", *Tunn. Undergr. Sp. Tech.*, **64**, 1-9.
- Han, L., Ye, G.L., Li, Y.H., Xia, X.H. and Wang, J.H. (2016), "In-situ monitoring of frost heave pressure during cross passage construction using ground freezing method", *Can. Geotech. J.*, **53**(3), 530-539.
- Hinchberger, S., Weck, J. and Newson, T. (2010), "Mechanical and hydraulic characterization of plastic concrete for seepage cut-off walls", *Can. Geotech. J.*, **47**(4), 461-471.
- Hugman, R., Stigter, T.Y., Monteiro, J.P., Costa, L. and Nunes, L.M. (2015), "Modeling the spatial and temporal distribution of coastal groundwater discharge for different water use scenarios under epistemic uncertainty: Case study in South Portugal", *Environ. Earth Sci.*, **73**(6), 2657-2669.
- Jiao, J.J., Leung, C.M. and Ding, G.P. (2008), "Changes to the groundwater system, from 1888 to present, in a highly-urbanized coastal area in Hong Kong, China", *Hydrogeol. J.*, **16**(8), 1527-1539.
- Jiao, J.J., Wang, X.S. and Nandy, S. (2006), "Preliminary assessment of the impacts of deep foundations and land reclamation on groundwater flow in a coastal area in Hong Kong, China", *Hydrogeol. J.*, **14**(1-2), 100-114.
- Jin, Y.F., Yin, Z.Y., Shen, S.L. and Hicher, P.Y. (2016a), "Selection of sand models and identification of parameters using an enhanced genetic algorithm", *J. Numer. Anal. Met. Geomech.*, **40**(8), 1219-1240.
- Jin, Y.F., Yin, Z.Y., Shen, S.L. and Hicher, P.Y. (2016b), "Investigation into MOGA for identifying parameters of a critical state based sand model and parameters correlation by factor analysis", *Acta Geotech.*, **11**(5), 1131-1145.
- Johnson, G.S., Frederick, D.B. and Cosgrove, D.M. (2002), "Evaluation of a pumping test of the Snake River Plain aquifer using axial-flow numerical modeling", *Hydrogeol. J.*, **10**(3), 428-437.
- Li, S.J., Liu, Y.X. and Wang, D.G. (2002), "Inversion and project application of rock permeability coefficient based on neural network", *Chin. J. Rock Mech. Eng.*, **21**(4), 479-483 (in Chinese).
- Lin, H.T., Tan, Y.C., Chen, C.H., Yu, H.L., Wu, S.C. and Ke, K.Y. (2010), "Estimation of effective hydrogeological parameters in heterogeneous and anisotropic aquifers", *J. Hydrol.*, **389**(1-2), 57-68.
- Liu, J. and Wang, Y. (2003), "Improved genetic algorithm in back analysis for seepage parameters of fissured rock masses", *Rock Soil Mech.*, **24**(2), 237-241 (in Chinese).
- Ma, L., Xu, Y.S., Shen, S.L. and Sun, W.J. (2014), "Evaluation of the hydraulic conductivity of aquifers with piles", *Hydrogeol. J.*, **22**(2), 371-382.
- Mulligan, C.N., Yong, R.N. and Gibbs, B.F. (2001), "Remediation technologies for metal-contaminated soils and groundwater: An evaluation", *Eng. Geol.*, **60**(1), 193-207.
- Ni, J.C., Cheng, W.C. and Ge, L. (2011), "A case history of field pumping tests in a deep gravel formation in the Taipei Basin, Taiwan", *Eng. Geol.*, **117**(1-2), 17-28.
- Ni, J.C., Cheng, W.C. and Ge, L. (2013), "A simple data reduction method for pumping tests with tidal, partial penetration, and storage effects", *Soil. Found.*, **53**(6), 894-902.
- Pujades, E., Carrera, J., Vázquez-Suñé, E., Jurado, A., Villarrasa, V. and Mascuñano-Salvador, E. (2012b), "Hydraulic characterization of diaphragm walls for cut and cover

- tunnelling”, *Eng. Geol.*, **125**, 1-10.
- Pujades, E., López, A., Carrera, J., Vázquez-Suñé, E. and Jurado, A. (2012a), “Barrier effect of underground structures on aquifers”, *Eng. Geol.*, **145**, 41-49.
- Pujades, E., Vázquez-Suñé, E., Carrera, J. and Jurado, A. (2014), “Dewatering of a deep excavation undertaken in a layered soil”, *Eng. Geol.*, **178**, 15-27.
- Ranjan, S., Mysore, S.N., Kenneth, L.M. and Gordon, P.B. (2008), “Investigations of pile foundations in brownfields”, *J. Geotech. Geoenviron. Eng.*, **134**(10), 562-572.
- Renard, P. and Marsily, G.D. (1997), “Calculating equivalent permeability: A review”, *Adv. Water Resour.*, **20**(5-6), 253-278.
- Richardson, J.P. and Nicklow, J.W. (2002), “In situ permeable reactive barriers for groundwater contamination”, *Soil Sediment Contam.*, **11**(2), 241-268.
- Schöniger, A., A. Illman, W., Wöhling, T. and Nowak, W. (2015), “Finding the right balance between groundwater model complexity and experimental effort via Bayesian model selection”, *J. Hydrol.*, **531**(1), 96-110.
- Shanghai Urban Construction and Communications Commission (SUCCC) (2010), Foundation Design Code (DGJ08-11-2010).
- Shen, S.L. and Xu, Y.S. (2011), “Numerical evaluation of land subsidence induced by groundwater pumping in Shanghai”, *Can. Geotech. J.*, **48**(9), 1378-1392.
- Shen, S.L., Wang, J.P., Wu, H.N., Xu, Y.S. and Ye, G.L. (2015b), “Evaluation of hydraulic conductivity for both marine and deltaic deposits based on piezocone testing”, *Ocean Eng.*, **110**, 174-182.
- Shen, S.L., Wang, Z.F., Yang, J. and Ho, E.C. (2013), “Generalized approach for prediction of jet grout column diameter”, *J. Geotech. Geoenviron.*, **139**(12), 2060-2069.
- Shen, S.L., Wu, H.N., Cui, Y.J. and Yin, Z.Y. (2014), “Long-term settlement behavior of metro tunnels in the soft deposits of Shanghai”, *Tunn. Undergr. Sp. Tech.*, **40**, 309-323.
- Shen, S.L., Wu, Y.X., Xu, Y.S., Hino, T. and Wu, H.N. (2015a), “Evaluation of hydraulic parameters from pumping tests in multi-aquifers with vertical leakage in Tianjin”, *Comput. Geotech.*, **68**, 196-207.
- Tan, Y. and Lu, Y. (2016a), “Why excavation of a small air shaft caused excessively large displacements: Forensic investigation”, *J. Perform. Constr. Fac.*, **31**(2), 04016083.
- Tan, Y. and Wang, D.L. (2013a), “Characteristics of a large-scale deep foundation pit excavated by central-island technique in Shanghai soft clay. I: Bottom-up construction of the central cylindrical shaft”, *J. Geotech. Geoenviron.*, **139**(11), 1875-1893.
- Tan, Y. and Wang, D.L. (2013b), “Characteristics of a large-scale deep foundation pit excavated by central-island technique in Shanghai soft clay. II: top-down construction of the peripheral rectangular pit”, *J. Geotech. Geoenviron.*, **139**(11), 1894-1910.
- Tan, Y., Huang, R., Kang, Z. and Bin, W. (2016b), “Covered semi-top-down excavation of subway station surrounded by closely spaced buildings in downtown Shanghai: Building response”, *J. Perform. Constr. Fac.*, **30**(6), 04016040.
- Vilarrasa, V., Carrera, J., Jurado, A., Pujades, E. and Vázquez-Suñé, E. (2011), “A methodology for characterizing the hydraulic effectiveness of an annular low-permeability barrier”, *Eng. Geol.*, **120**(1-4), 68-80.
- Wang, J.X., Feng, B., Liu, Y., Wu, L.G., Zhu, Y.F., Zhang, X.S., Tang, Y.Q. and Yang, P. (2012), “Controlling subsidence caused by de-watering in a deep foundation pit”, *Bull. Eng. Geol. Environ.*, **71**(3), 545-555.
- Wang, J.X., Feng, B., Yu, H., Guo, T., Yang, G. and Tang, J. (2013), “Numerical study of dewatering in a large deep foundation pit”, *Environ. Earth Sci.*, **69**(3), 863-872.
- Wu, C.J., Ye, G.L., Zhang, L.L., Bishop, D. and Wang, J.H. (2014), “Depositional environment and geotechnical properties of Shanghai clay: A comparison with Ariake and Bangkok clays”, *Bull. Eng. Geol. Environ.*, **74**(3), 717-732.
- Wu, H.N., Shen, S.L., Liao, S.M. and Yin, Z.Y. (2015b), “Longitudinal structural modelling of shield tunnels considering shearing dislocation between segmental rings”, *Tunn. Undergr. Sp. Tech.*, **50**, 317-323.
- Wu, H.N., Shen, S.L., Ma, L., Yin, Z.Y. and Horpibulsuk, S. (2015a), “Evaluation of the strength increase of marine clay under staged embankment loading: A case study”, *Mar. Georesour. Geotechnol.*, **33**(6), 532-541.
- Wu, S.C., Tan, Y.C., Chen, C.H. and Lin, H.T. (2013), “Estimation of effective hydrogeological parameters by considering varying heterogeneity and pumping rates”, *Environ. Earth Sci.*, **68**(1), 169-180.
- Wu, Y.X., Shen, S.L. and Yuan, D.J. (2016), “Characteristics of dewatering induced drawdown curve under blocking effect of retaining wall in aquifer”, *J. Hydrol.*, **539**, 554-566.
- Wu, Y.X., Shen, S.L., Wu, H.N., Xu, Y.S., Yin, Z.Y. and Sun, W.J. (2015c), “Environmental protection using dewatering technology in a deep confined aquifer beneath a shallow aquifer”, *Eng. Geol.*, **196**, 59-70.
- Wu, Y.X., Shen, S.L., Xu, Y.S. and Yin, Z.Y. (2015d), “Characteristics of groundwater seepage with cut-off wall in gravel aquifer. I: Field observations”, *Can. Geotech. J.*, **52**(10), 1526-1538.
- Wu, Y.X., Shen, S.L., Yin, Z.Y. and Xu, Y.S. (2015e), “Characteristics of groundwater seepage with cut-off wall in gravel aquifer. II: Numerical analysis”, *Can. Geotech. J.*, **52**(10), 1539-1549.
- Xu, Y.S., Shen, S.L., Du, Y.J., Chai, J.C. and Horpibulsuk, S. (2013), “Modelling the cutoff behavior of underground structure in multi-aquifer-aquitard groundwater system”, *Nat. Hazards*, **66**(2), 731-748.
- Xu, Y.S., Ma, L., Shen, S.L. and Sun, W.J. (2012), “Evaluation of land subsidence by considering underground structures penetrated into aquifers of Shanghai”, *Hydrogeol. J.*, **20**(8), 1623-1634.
- Xu, Y.S., Shen, S.L. and Du, Y.J. (2009), “Geological and hydrogeological environment in Shanghai with geohazards to construction and maintenance of infrastructures”, *Eng. Geol.*, **109**(3-4), 241-254.
- Xu, Y.S., Shen, S.L., Ma, L., Sun, W.J. and Yin, Z.Y. (2014), “Evaluation of the blocking effect of retaining walls on groundwater seepage in aquifers with different insertion depths”, *Eng. Geol.*, **183**, 254-264.
- Xu, Y.S., Shen, S.L., Ren, D.J. and Wu, H.N. (2016), “Analysis of factors in land subsidence in Shanghai: A view based on a strategic environmental assessment”, *Sustain.*, **8**(6), 573.
- Ye, G.L. and Ye, B. (2016), “Investigation of the overconsolidation and structural behavior of Shanghai clays by element testing and constitutive modeling”, *Undergr. Sp.*, **1**(1), 62-77.
- Ye, G.L., Hashimoto, T., Shen S.L., Zhu H.H. and Bai T.H. (2015), “Lessons learnt from unusual ground settlement during Double-O-Tube tunnelling in soft ground”, *Tunn. Undergr. Sp. Tech.*, **49**, 79-91.
- Yin Z.Y., Zhu, Q.Y., Yin, J.H. and Ni, Q. (2014), “Stress relaxation coefficient and formulation for soft soils”, *Géotech. Lett.*, **4**(1), 45-51.
- Yin, Z.Y., Hicher, P.Y., Dano, C. and Jin Y.F. (2016), “Modeling the mechanical behavior of very coarse granular materials”, *J. Eng. Mech.*, **143**(1), C4016006.
- Yin, Z.Y., Yin, J.H. and Huang, H.W. (2015), “Rate-dependent and long-term yield stress and strength of soft Wenzhou marine clay: experiments and modeling”, *Mar. Georesour. Geotech.*, **33**(1), 79-91.
- Yoon, S., Lee, S.R., Kim, Y.T. and Go, G.H. (2015), “Estimation of saturated hydraulic conductivity of Korean weathered granite soils using a regression analysis”, *Geomech. Eng.*, **9**(1), 101-

113.

- Zhang, D.M., Huang, Z.K., Yin, Z.Y., Ran, L. and Huang, H.W. (2017), "Predicting the grouting effect on leakage-induced tunnels and ground response in saturated soils", *Tunn. Undergr. Sp. Tech.*, **65**, 76-90.
- Zhang, N., Shen, S.L., Wu, H.N., Chai, J.C. and Yin, Z.Y. (2015), "Evaluation of effect of basal geotextile reinforcement under embankment loading on soft marine deposits", *Geotext. Geomembr.*, **43**(6), 506-514.
- Zhou, A.N., Sheng, D. and Carter, J.P. (2012), "Modelling the effect of initial density on soil-water characteristic curves", *Geotechnique*, **62**(8), 669-680.
- Zhou, N., Vermeer, P.A., Lou, R., Tang, Y. and Jiang, S. (2010), "Numerical simulation of deep foundation pit dewatering and optimization of controlling land subsidence", *Eng. Geol.*, **114**(3), 251-260.
- Zhou, X. (2016), "Estimation of the position of the sharp interface in littoral aquifers with hydraulic head differences within the fresh-water zone", *Environ. Earth Sci.*, **75**(2), 110.
- Zhu, Q.Y., Yin, Z.Y., Hicher, P.Y. and Shen, S.L. (2016), "Nonlinearity of one-dimensional creep characteristics of soft clays", *Acta Geotech.*, **11**(4), 887-900.

CC